Finite Frequency Group Velocity Sensitivity Kernels for Surface Wave Tomography

M.P. Barmin, M.H. Ritzwoller, and A.L. Levshin

University of Colorado at Boulder

Summary & Conclusions

Observed surface wave group-delays depend both on relative phase speed and relative group speed. This dual-dependence can be expressed principally in two different ways. We ask two questions.

(a) Is one of the two formulations preferable over the other?
(b) Does either or both of the formulations provide a firm foundation for group-delay tomography?

From forward simulations and tomography with real data, we conclude the following:

(1) Although the group speed kernels in the two formulations differ strongly in their side-lobes, both formulations provide equally valid bases for group-delay tomography.
(2) At and below 100 sec period, the phase speed terms contribute only about 10% of the group delay-times which is well below data misfit. The phase speed integrals can be safely ignored at these periods.
(3) At periods above 100 sec, observed group-delays should be corrected for the phase speed integral using a 3D model or an empirical scaling relation between the relative group and phase speeds.
(4) Correcting for the phase speed terms using a 3D model or an empirical scaling relationship between group and phase speeds should improve the resulting maps at all periods, but the effect will be small at and below 100 sec period.

Theory

Adopting the notation of Dahlen and Zhou (2005), which itself follows the notation of Zhou et al. (2004), the dual-dependence of group delay $\delta t(\omega)$ on group and phase speed perturbations is written:

term A   term B

$$\delta t \;=\; \iint_\Omega K_t^U \left(\frac{\delta U}{U}\right) d\Omega + \iint_\Omega K_t^c \left(\frac{\delta c}{c}\right) d\Omega, \qquad (1)$$

where $\delta c/c$ is the relative phase speed perturbation, $\delta U/U$ is the relative group speed pertubation, and both depend on frequency. K_t^U and K_t^c are the group and phase speed Fréchet sensitivity kernels for which Dahlen and Zhou (2005) provide explicit forms.

The dependence of group delay on group and phase speeds given in equation (1) is not unique. Using the following relation

$$\frac{\delta c}{c} = \frac{\delta U}{U} - kU\frac{\partial}{\partial \omega}\left(\frac{\delta c}{c}\right) \qquad (2)$$

we can replace relative phase speed with the difference between relative group speed and the dimensionless frequency derivative of relative phase speed:

term C   term D

$$\delta t \;=\; \iint_\Omega \tilde{K}_t^U \left(\frac{\delta U}{U}\right) d\Omega + \iint_\Omega \tilde{K}_t^{c'} \left[\omega\frac{\partial}{\partial \omega}\left(\frac{\delta c}{c}\right)\right] d\Omega \qquad (3)$$

$$\tilde{K}_t^U \;=\; K_t^c + K_t^U \qquad (4)$$

$$\tilde{K}_t^{c'} \;=\; -\left(\frac{U}{c}\right) K_t^c \qquad (5)$$

Sensitivity Kernels

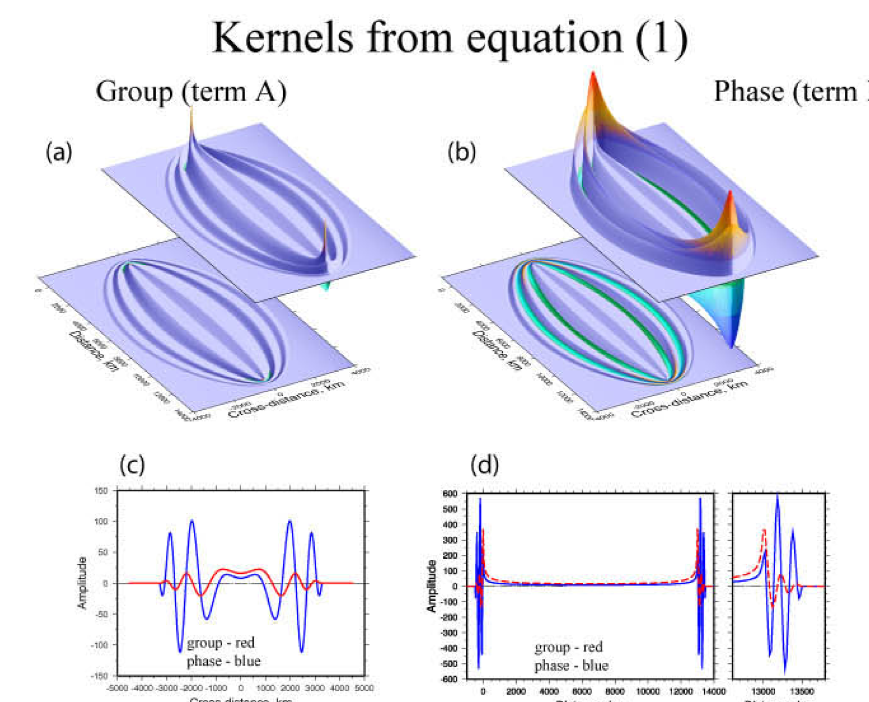

Figure 1. Example Rayleigh wave Frechet sensitivity kernels from equation (1) for an epicentral distance of 13,000 km at 100 sec period. (a) Group delay kernel from equation (1). (b) Phase delay kernel from equation (1). (c) Central cross-section of the group delay kernel (red line) and the phase delay kernel (blue line) across the kernels perpendicular to the line linking the source and receiver. (d) Profile of the group (red line) and phase (blue line) delay kernels along the line linking source and receiver, with a blow-up near the end of the kernels.

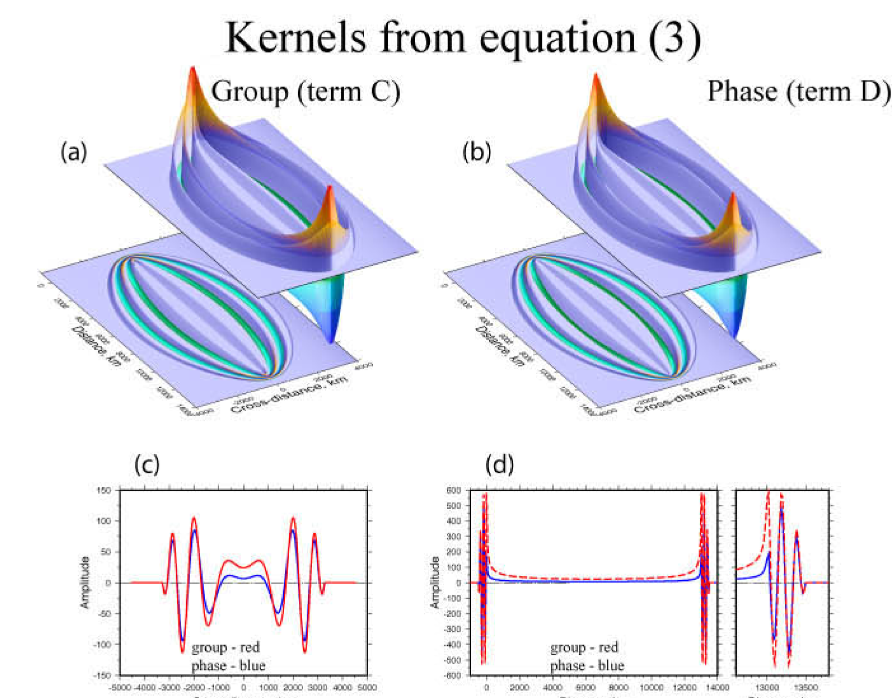

Figure 2. Example Rayleigh wave Frechet sensitivity kernels from equation (3) for an epicentral distance of 13,000 km at 100 sec period. (a) Group delay kernel from equation (3). (b) Phase delay kernel from equation (3) (sign-reversed for comparison). (c) Central cross-section of the group delay kernel (red line) and the sign-reversed phase delay kernel (blue line) across the kernels perpendicular to the line linking the source and receiver. (d) Profile of the group (red line) and sign-reversed phase (blue line) dela y kernels along the line linking source and receiver, with a blow-up near the end of the kernels.

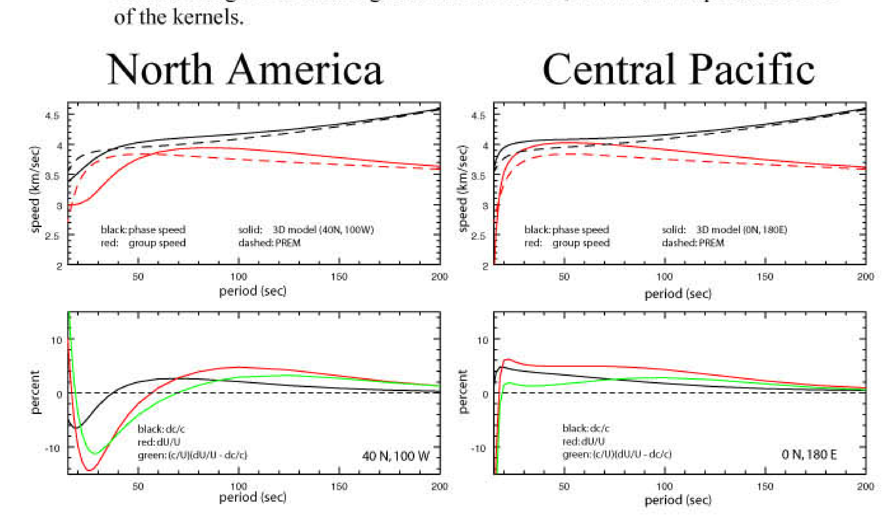

Figure 3. (TOP) Dispersion curves. Rayleigh wave group and phase speed curves for PREM compared (LEFT) with a typical location within a continent and (RIGHT) within an ocean. Black lines are phase speed and red lines are group speed. Dashed lines are from PREM and solid lines are from a recent 3D model (Shapiro and Ritzwoller, 2002) computed in the central U.S. (40N, 100W) and central Pacific (0N, 180E). (BOTTOM) Relative structural perturbations. Relative phase speed (black), relative group speed (red), and the dimensionless frequency derivative of relative phase speed (green) computed using the 3D model at (LEFT) (40N, 100W) and (RIGHT) (0N, 180E).

Figures 1 and 2 give examples of the relative shapes and amplitudes of the group and phase velocity sensitivity kernels in equations (1) and (3). The relative smallness of the side-lobes of the group speed kernel compared with the phase speed kernel in equation (1) was noted by Dahlen and Zhou (2005). The reformulation of the theory given by equation (3), produces sensitivity kernels whose side-lobes are commensurable. This gives the impression that the reformulation may be preferable over the version given by equation (1). As shown at right, however, both formalisms provide equally valid bases for group velocity tomography.

With either formulation (eq. (1) or (3)) of the dependence of group-delayon group and phase speeds, the group speed kernel is larger in the principal lobe of the sensitivity kernel than the phase speed kernel. The delay-time produced by each term in equations (1) and (3) will depend on the integrated effect of the side-lobes in the sensitivity kernels and the relative size of the relative group and phase perturbations and the dimensionless frequency derivative of relative phase speed. The integrated effect of the side-lobes can be determined by forward simulations (see panel below) and tomography with real data (see panels at right).

Figure 3 shows that the relative group speed is expected to be, on average, about twice the size of the relative phase speed, and the dimensionless frequency derivative of relative phase speed is expected to be about intermediate in size between them. These quantities vary with frequency and near zero-crossings shuffle their relative sizes.

Group-Delay Simulation

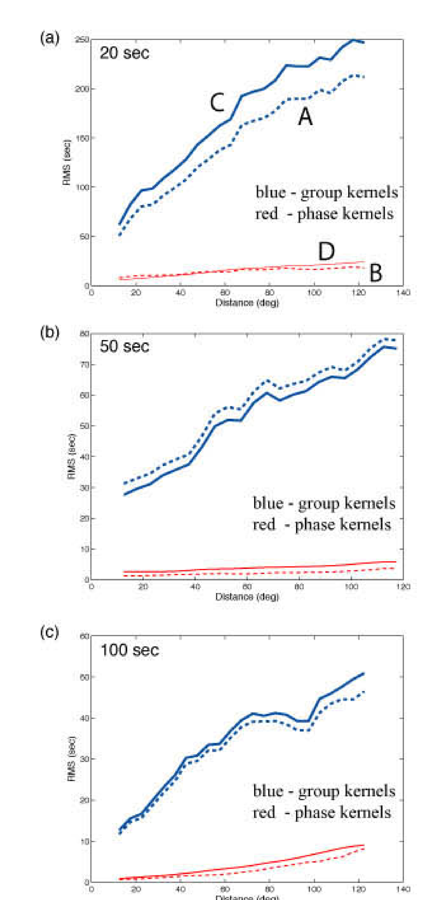

Figure 4. Summary results of the delay time simulation. RMS of each of the four travel time integrals in equations (1) and (3) computed through the 3D model of Shapiro and Ritzwoller (2002) using the paths from the CU group velocity data set, plotted as a function of epicentral distance in equatorial degrees. The BLUE lines (with large values) are the group speed integrals and the RED lines (with small values) are the phase speed integrals. The solid lines correspond to the integrals in equation (3) and the dashed lines are for the integrals in equation (1).

To determine the relative delay-time contribution of the group and phase speed integrals in equations (1) and (3), simulations are performed using a 3D model of the crust and upper mantle (Shapiro and Ritzwoller, 2002). Using paths from the CU data set of measured group velocities, the four integrals (terms A, B, C, and D) in equations (1) and (3) are computed. Results are shown in Figure 4 (at left) which presents the RMS of each integral as a function of epicentral distance. The RMS size averaged over epicentral distance is shown in Table 1 below. At periods of 100 sec and below, the phase speed terms in equations (1) and (3) contribute only about 10% of the total travel time signal, contributing about 1/4 of the data misfit. There are significantly larger sources of error to contend with in group velocity tomography than neglect of the phase terms in equations (1) and (3) at periods of 100 sec and below. At 150 sec, however, the neglect of the phase term may contribute as much as half the data misfit.

Table 1. RMS of the four integrals in equations (1) and (3) taken through the 3D model of Shapiro and Ritzwoller (2002) using paths from a real data set, averaged over epicentral distance out to 120°. Column A is $\iint_\Omega K_t^U\,(\delta U/U)\,d\Omega$, column B is $\iint_\Omega K_t^c\,(\delta c/c)\,d\Omega$, column C is $\iint_\Omega \tilde{K}_t^U\,(\delta U/U)\,d\Omega$, and column D is $\iint_\Omega \tilde{K}_t^{c'}\,[\omega(\partial/\partial\omega)\,(\delta c/c)]\,d\Omega$. Ratios of the columns are rounded and presented in percent. Misfit is rms misfit in tomography with real data.

period (sec)	A (sec)	B (sec)	B/A (%)	C (sec)	D (sec)	D/C (%)	misfit (sec)
20	144.4	14.3	10	170.1	14.7	8	43
50	59.3	2.3	4	56.1	3.9	7	17
100	36.2	3.8	11	38.3	4.8	12	17
150	30.3	6.9	23	33.5	10.0	30	20

Tomography with Different Theories

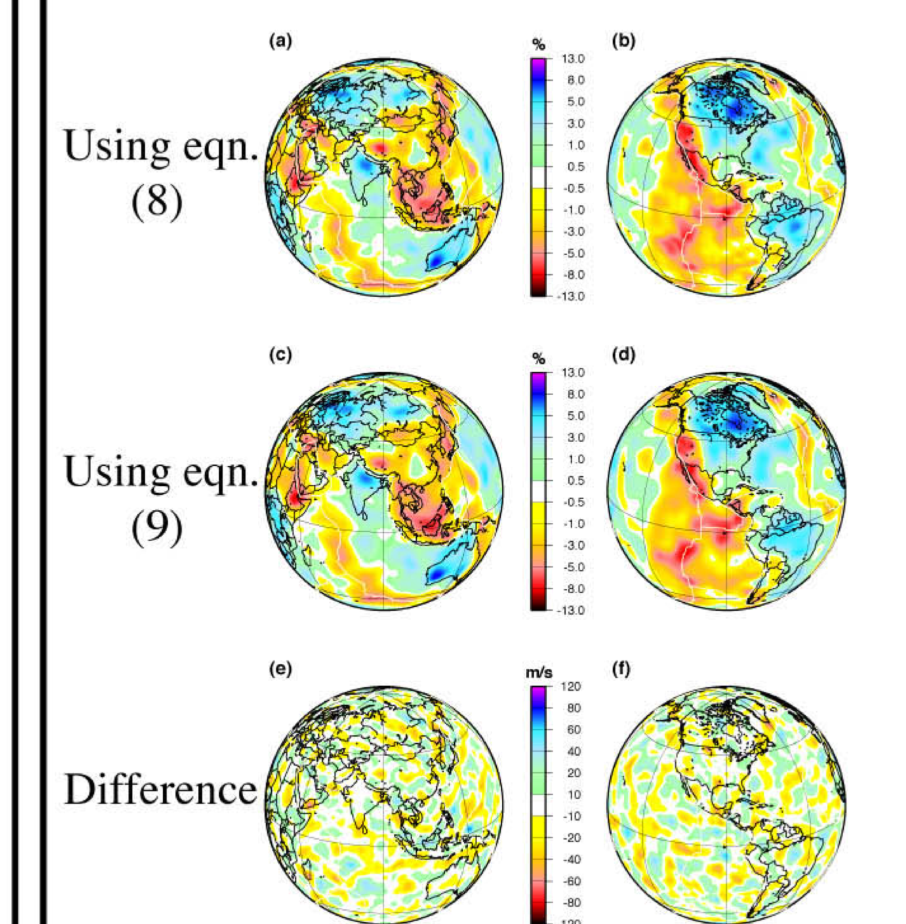

Figure 5. Tomography based on equation (8) compared with tomography based on equation (9). In both cases, the phase integral correction has been made by using the 3D model of Shapiro and Ritzwoller (2002).
(a) - (b) Results using equation (8). (c) - (d) Results using equation (9).
(e) - (f) Difference between the maps estimated with the two theories.
The RMS of the difference maps is about 19 m/s or about 0.5%, implying that the maps are practically the same. These results are for 100 sec Rayleigh waves.

Either equations (1) or (3) can be the basis for tomography, either directly:

$$\delta t \;\sim\; \iint_\Omega K_t^U \left(\frac{\delta U}{U}\right) d\Omega \qquad (6)$$

$$\delta t \;\sim\; \iint_\Omega \tilde{K}_t^U \left(\frac{\delta U}{U}\right) d\Omega \qquad (7)$$

or by correcting for the phase term using a 3D model:

$$\delta t' = \delta t - \iint_\Omega K_t^c \left(\frac{\delta c}{c}\right) d\Omega \;\sim\; \iint_\Omega K_t^U \left(\frac{\delta U}{U}\right) d\Omega \qquad (8)$$

$$\delta t' = \delta t - \iint_\Omega \tilde{K}_t^{c'} \left[\omega\frac{\partial}{\partial \omega}\left(\frac{\delta c}{c}\right)\right] d\Omega \;\sim\; \iint_\Omega \tilde{K}_t^U \left(\frac{\delta U}{U}\right) d\Omega \qquad (9)$$

Barmin et al. (2001) and Ritzwoller et al. (2002) present a method for surface wave tomography based on ray-theory or the use of spatially extended sensitivity kernels. Both equations (1) and (3) can form the basis for group delay tomography, either by truncating the phase terms (eqns. (6) and (7) above) or by correcting for the phase terms explicitly (eqns. (8) and (9)). We recommend using a 3D model to compute the phase terms and correct the observations accordingly. Alternately, a scaling relation between the relative group and phase speed perturbations could be used.

Figure 5 at left compares the results of group velocity tomography at 100 sec period using the two formalisms given by equations (8) and (9). In each case, the phase term has been computed using the 3D model of Shapiro and Ritzwoller (2002) and the phase correction has been applied to the observed group delay data. The maps differ only subtly. The differences that exist result principally from the different effect of damping in each case, as the inversion matrices differ.

These results imply that the two formulations given by equations (1) and (3) provide equally valid bases for group-delay tomography.

Results at 20 s, 50 s, 100 s Period:

The effect of neglecting the phase term

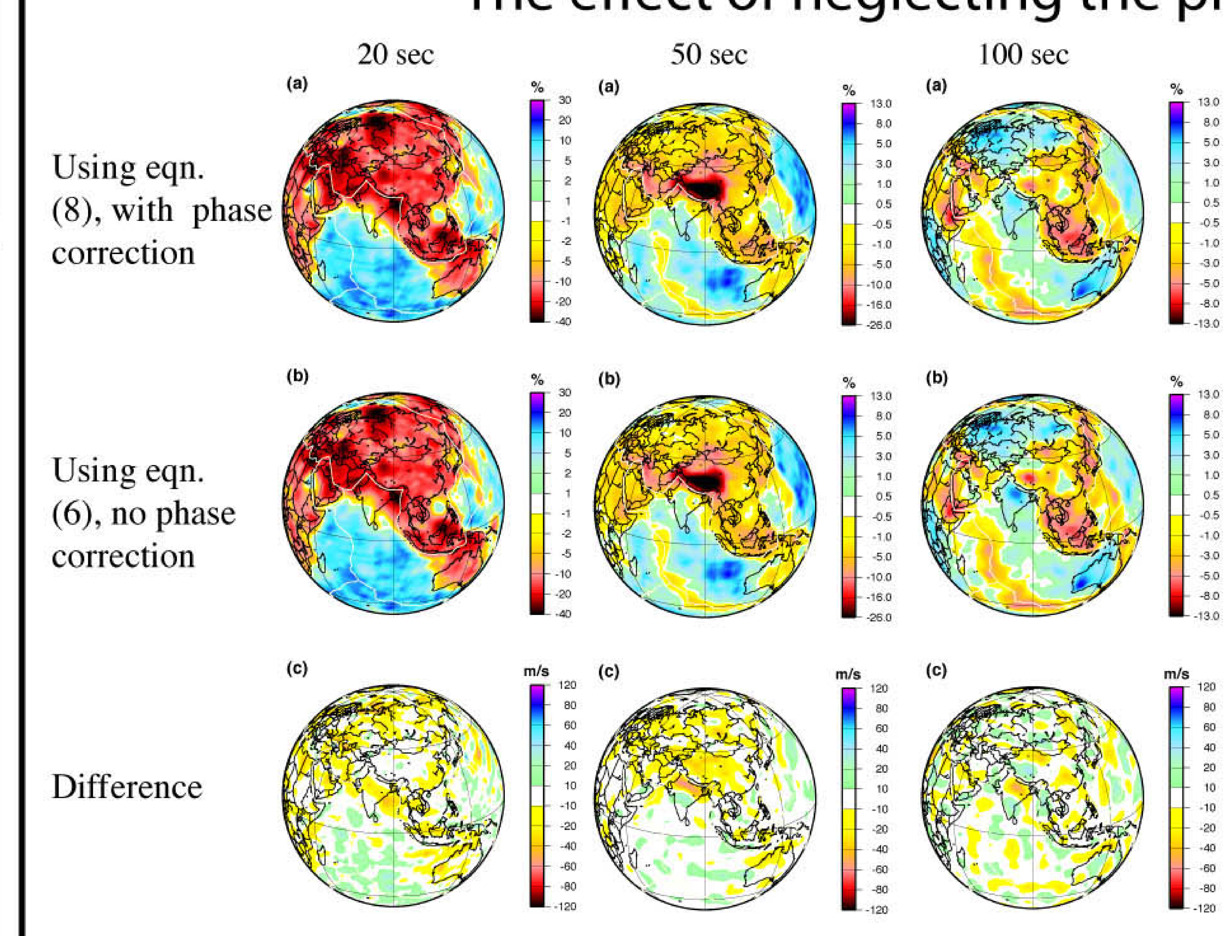

Figure 6. Comparison of tomographic maps estimated with equations (6) and (8) to determine the effect of ignoring the phase corrections. (LEFT) 20 sec period. (MIDDLE) 50 sec period. (RIGHT) 100 sec period. In each panel: (a) is the result using equation (8) with contains the phase correction, (b) is the result from equation (6) which does not include the phase corrections, and (c) is the difference between the resulting maps. The rms of the difference at 20 sec, 50 sec, and 100 sec is about 15 m/s, 10 m/s, and 13 m/s, respectively, or between 0.25% - 0.5%.

Although we recommend correcting the observed group-delays for the phase speed terms in equations (1) and (3), tomography can be performed without this correction. This is expressed by equations (6) and (7) above.

Tomography at 20 sec, 50 sec, and 100 sec at left demonstrates that completely ignoring the phase term has only a mild effect on the resulting group velocity maps at these periods. At 20 sec and 50 sec period, the maps are nearly indistinguishable with or without the phase term correction. At 100 sec period, differences between the maps are discernible but small.

At periods below 100 sec, therefore, the phase correction can be safely ignored, but at longer periods the phase correction should be made.

References

Barmin, M.P., M.H. Ritzwoller, and A.L. Levshin, A fast and reliable method for surface wave tomography, Pure Appl. Geophys., 151(8), 1351-1375, 2001.
Dahlen, F.A. and Ying Zhou, Surface-wave group-delay and attenuation kernels, Geophys. J. Int., in press, 2005.
Ritzwoller, M.H., N.M. Shapiro, M.P. Barmin, and A.L.Levshin, Global surface wave diffraction tomography, J. Geophys. Res., 107(B12), 2335, 2002.
Shapiro, N.M. and M.H. Ritzwoller, Monte-Carlo inversion for a global shear-velocity model of the crust and upper mantle, Geophys. J. Int., 151, 88-105, 2002.
Zhou, Y., F.A. Dahlen, and G. Nolet, Three-dimensional sensitivity kernels for surface wave observables, Geophys. J. Int., 158, 142-168, 2004.